Submitted to ApJ Letters

Chandra Observations of the Evolving Core of the Starburst Galaxy NGC 253

K. A. Weaver[1]

Laboratory for High Energy Astrophysics, NASA/Goddard Space Flight Center, Greenbelt, MD 20771, USA

kweaver@milkyway.gsfc.nasa.gov

T. M. Heckman and D. K. Strickland[2]

Johns Hopkins University, Department of Physics and Astronomy, Homewood campus, 3400 North Charles Street, Baltimore, MD 21218, USA

M. Dahlem[3]

European Southern Observatory, Casilla 19001 Santiago 19, CHILE

ABSTRACT

Chandra observations of the core of the nearby starburst galaxy NGC 253 reveal a heavily absorbed source of hard X-rays embedded within the nuclear starburst region. The source has an unabsorbed, 2 to 10 keV luminosity of $\geq 10^{39}$ erg s^{-1} and photoionizes the surrounding gas. We observe this source through a dusty torus with a neutral absorbing column density of $N_{\rm H} \sim 2 \times 10^{23}$ cm^{-2}. The torus is hundreds of pc across and collimates the starburst-driven nuclear outflow. We suggest that the ionizing source is an intermediate-mass black hole or a weakly accreting supermassive black hole, which may signal the beginnings or endings of AGN activity.

Subject headings: galaxies: nuclei - galaxies: active - galaxies: starburst - galaxies: NGC 253 - X-rays: galaxies

---

[1]also Johns Hopkins University

[2]Chandra Fellow

1. Introduction

In recent years, there has been increasing speculation about the connection between circumnuclear starbursts and active galactic nuclei (AGN). Such speculation is due mostly to the fact that, as our instruments allow us to probe closer to the cores of nearby galaxies, we find that an an increasing number contain starbursts and AGN in close proximity (Levenson, Weaver and Heckman 2001, and references therein). It is not clear whether proximity implies a physical connection, but a circumnuclear starburst could easily provide a pathway toward forming a supermassive black hole (and subsequent AGN), since it can processes as much as $\sim 10^{10}$ $M_\odot$ of material in $10^7 - 10^8$ years (Norman and Scoville 1988). To date, however, there has been little direct evidence for this scenario.

High-energy photons can penetrate the dense cores of nearby galaxies, and so X-ray observations are crucial for probing the possible links between starburst and AGN activity. For this purpose, we have obtained *Chandra* observations of the nearby ($\sim$ 2.6 Mpc) starburst galaxy NGC 253. In addition to possessing a strong circumnuclear starburst with a significant nuclear outflow (Strickland et al. 2000), there is also evidence for a weak AGN (Turner & Ho 1995, and more recently, Mohan, Anantharamaiah & Goss 2002). *Chandra*, with its resolution of $\sim 1''$ ($\sim$ 12 pc at NGC 253) allows us to untangle the X-ray emission processes of stellar and non-stellar activity for the first time at the core of the galaxy.

2. Data Analysis

The *Chandra* data were obtained with the CCD Imaging Spectrometer (ACIS) on 1999 December 16. The galaxy was placed on CCD chip S3 with the center of the galaxy placed at the focal-plane location that provides the best image quality. The absolute astrometric accuracy of the nuclear pointing is $< 1''$ rms.

Data reduction and analysis is performed using CIAO (version 2.1.3) and HEASOFT (version 5.1). The CCD focal-plane temperature during the NGC 253 observation was $-110°$ C. Accurate calibration files are not yet available for this mode[3], and so the data are re-processed instead with the latest (August 2001) gain-correction files. These are optimized for a focal-plane temperature of $-120°$ C (acisD2000...gainN0003.fits). The data are also screened to remove "bad" events, and time filtered to remove periods of high background. The remaining exposure time is 12,860 s. Spectral responses are created using the 2001 calibration files.

[3]see cxc.harvard.edu/cal/Links/Acis/acis/Cal_prods/matrix/matrix.html.

To assess systematic errors that might be introduced by using the $-120°$ calibration as opposed to a calibration optimized for a $-110°$ CCD temperature (not yet available), we carefully examined two archived pointings of NGC 1068 taken in both temperature modes. Processing and comparing the data sets with the April 2000, $-110°$ and $-120°$ gain files, and the August 2001 $-120°$ and gain files, we find that using the detector gain and resolution available in 2001 is superior to any of the 2000 calibration. Furthermore, any errors that are introduced by using the 2001 $-120°$ calibration (as opposed to a yet unavailable, revised $-110°$ calibration) are only $\sim 20 - 30\%$ in resolution and efficiency and are concentrated below 1 keV, a portion of the spectrum that we do not investigate here.

The X-ray spectrum of the galaxy core contains ~ 580 photons, which is adequate for fitting spectral models if the data are properly binned as a function of energy. On the other hand, the narrow spectral features are better seen in the unbinned data. We therefore examine both the binned and the unbinned spectrum, using the statistical techniques of χ^2 and the c-statistic, respectively. The former technique allows us to determine the overall goodness of fit for continuum models while the latter provides details about the emission lines.

3. The ACIS Image

A three color composite *Chandra* image of the central $1.7' \times 2'$ (1.4 x 1.6 kpc) region of NGC 253 is shown in Figure 1. The cross marks the position of the compact radio nucleus (Turner and Ho 1985), which is assumed to lie at the core of the galaxy. The colors have been optimized with energy to best show the hard X-ray, arc-shaped feature (seen in green) that lies along the plane of the galaxy. This feature has not before been imaged in X-rays. The arc is approximately $5''$ by $23''$ (60 pc by 300 pc) and its color indicates significant foreground absorption of soft X-rays.

Figure 2 shows a closer view of the central region of the galaxy ($26''$ by $37''$) in the three energy bands that make up Figure 1. The dashed black line marks the location of an extended region of radio emission, which is interpreted as a $\sim 60 \times 300$ pc rotating, dusty torus (Israel, White and Baas 1995, Dahlem et al. in prep.). The X-ray spectrum of the galaxy core indicates an absorbing column density through the torus of $N_{\rm H} = 10^{23}$ cm^{-2}, which is consistent with the H_2 column densities deduced from the interferometer maps of this region (Frayer, Seaquist and Frail 1998, Peng et al. 1996). The position of the arc with respect to the outflow suggests that the torus is the collimating mechanism for the outflow, and so we will refer to it throughout the rest of the paper as the collimating torus. The inner edge of the collimating torus is traced by a loop of optical/IR sources (red symbols in Figure

2), while OH maser and compact radio sources mark a nuclear ridge of star formation in the dense regions where the gas piles up as it orbits in the bar potential (Peng et al. 1996).

The hard X-ray emission, while partly extended along the nuclear ridge and coincident with the radio and maser sources, is confined to a relatively small, 5″ ($\sim$ 50 pc) area inside this cavity. It is not clear whether the peak in hard X-ray emission is truly point like, but it is coincident with the compact synchrotron source at the center of the galaxy, which has a flat radio spectrum ($\alpha = 0.04 \pm 0.06$) and a brightness temperature of $T_b \sim 10^5$ K. This temperature is too high to be due to free-free emission from H II regions, but is within the upper limit for the brightness temperature in starbursts (Condon et al. 1991). On the other hand, hints of a non-starburst origin are found from observations of radio recombination line emission, which implies the presence of a source of ionizing radiation with a flux of $6 - 20 \times 10^{51}$ photons s^{-1} (Mohan, Anantharamaiah & Goss (2002).

We note that the *Chandra* data are not sensitive to the hard X-ray emission on much larger scales, such as that observed with XMM (Pietsch, et al. 2000).

4. The Nuclear Spectrum

The nuclear spectrum is extracted from within a circular region of diameter 5″ centered 1″ to the northeast of the radio nucleus (to avoid contamination from a young star cluster associated with the peak in the medium X-ray image in Figure 2b). Using a standard binning for the data tends to smooth out some of the sharper features in the spectrum and so to examine individual features we use the unbinned spectrum. The results of Gaussian fits to the emission lines are listed in Table 1. All lines are detected with a confidence level of $\geq$ 90% according to an F-test. The core spectrum, binned for illustration purposes, is shown in Figure 3a.

He-like triplets of Mg, Si and S indicate a strong contribution from an optically thin plasma. However, the line equivalent widths are unusually large and inconsistent with a thermal gas with solar abundance ratios for a plasma in ionization equilibrium (Mewe et al. 1985; Kaastra 1992; Liedahl, Osterheld and Goldstein 1995). This is borne out by the binned spectrum, which cannot be fitted with single or multi-temperature thermal plasma models with solar abundances (Models 1, 2, and 3, Table 2). When the high-temperature Mekal component is replaced with a power law having the same absorption as the low temperature Mekal component (Model 4), an excellent fit is obtained (χ^2_ν=1.03). The problem is that the photon index of -0.3 is much smaller than observed for any known type of X-ray emitter. Allowing a second, larger absorbing column in front of the high-energy component, results

in more realistic descriptions of the spectrum. In this case the hard component can be a thermal plasma with solar abundances (Model 5) or a power law with reasonable values of $\Gamma = 1.4 - 1.9$, as might be expected for an AGN or XRBs (Model 6). For Model 6 the best-fitting absorbing column density is $N_{\rm H} \sim 2 \times 10^{23}$ cm^{-2} and the unabsorbed $2 - 10$ keV luminosity is 2×10^{39} erg s^{-1}.

Although the binned spectrum is statistically well described by models 5 or 6, the features between 3 and 6 keV that show up prominently in the unbinned data are not predicted by either model. We have verified that similar features exist in the archived XMM data and so we are confident that they are real. Such features are presumably due to Ar and Ca, and are predicted at or near their observed energies for a highly photoionized plasma (Bautista & Kallman 2000). We therefore added another component to our model; this one representing emission from a spherical distribution of clouds with density 10^9 cm^{-3} that fully cover a central, power-law source with $\Gamma \sim 1.9$. The model was generated with *xstar* (heasarc.gsfc.nasa.gov/docs/software/xstar), and represents conditions similar to the core of a Seyfert 1 galaxy (T. Yaqoob, private communication). With this component in the model, we find an excellent match to the unbinned spectrum. The final, best-fitting model is a three-component hybrid plasma model, consisting of a moderately-absorbed, low-temperature Mekal plasma plus a heavily-absorbed power law and emission from a photoionized plasma with ionization parameter $\xi \sim 700$ (Figure 3b). The results from fitting this model to the binned spectrum are listed in Table 2 (Model 7) for easy comparison with earlier fits.

5. The Nature of the Hard X-ray Source

Our analysis of the *Chandra* data suggests the presence of a significant source of photoionization at the center of the nearby galaxy NGC 253. This result compliments the recent discovery of resolved, (FWHM$\sim$ 200 km s^{-1}) radio recombination line emission at the same location by Mohan et al. (2002). These authors rule out a compact SNR and young star cluster as the ionizing source. Similarly, we find such sources implausible because they would produce a softer ionizing X-ray spectrum than observed. We therefore consider other plausible sources of hard X-rays.

5.1. Inverse-Compton Emission

We can estimate the contribution of inverse Compton emission in NGC 253 following the arguments in Moran, Lehnert, & Helfand (1999). The ratio of the inverse Compton and synchrotron luminosities (L_{IVC}/L_S) is given by the ratio of the energy density in the seed photon field to the energy density in the magnetic field. To estimate the former, we first use the well-known radio-infrared correlation for star-forming galaxies (Condon 1992) and the high resolution 20-cm VLA radio map from Ulvestad & Antonucci (1997) to deduce that the far-infrared luminosity of the central-most 5 arcsec in NGC 253 is 5×10^{42} erg s^{-1}. Adopting the mean bolometric correction of 1.75 measured for dusty starburst galaxies by Calzetti et al. (2000), the bolometric surface-brightness of the nucleus of NGC 253 is then $B_{bol} = 320$ erg cm^{-2} s^{-1} and the radiant energy density is $U_{rad} \sim B_{bol}/c = 1.1 \times 10^{-8}$ erg cm^{-3}. To estimate the energy density in the magnetic field, we apply standard minimum-energy assumptions to the VLA 20cm radio data. We take Condon's (1992) equation 13 with $\beta = 40$ (the galactic value for the proton/electron energy ratio) and a path length of 60 pc (5 arcsec). This implies a magnetic field strength of 270 μG and an energy density $U_B = B^2/8\pi = 2.8 \times 10^{-9}$ erg cm^{-3}.

Thus, we estimate that $L_{IVC}/L_S = 3.8$. At 20 cm, the monochromatic power of the central 5 arcsec is $\nu P_\nu = 7.5 \times 10^{36}$ erg s^{-1}, while the corresponding power at 4.5 keV is 1.2×10^{39} erg s^{-1}. This suggests that the inverse Compton process makes only a minor contribution to the hard X-ray emission. However, we emphasize that our estimate is rough and depends on the assumption of minimum energy conditions. Within the context of our simple estimate, a dominant inverse Compton contribution to the hard X-rays seemingly requires that the magnetic field strength is about a factor of 7 below the minimum-energy value.

5.2. An Evolved Starburst

The nuclear starburst in NGC 253 is approximately 20 to 30 million years old (Engelbracht et al. 1998), which implies that its hard X-ray emission is dominated by XRBs (Van Bever & Vanbeveren 2000). XRBs naturally produce hard X-ray spectra, and only a handful of bright XRBs would be required to produce the observed $2-10$ keV luminosity of 2×10^{39} erg s^{-1} (Grimm, Gilfanov & Sunyaev 2001). On the other hand, equivalent widths of the emission lines are tens to hundreds of times larger than those of Galactic XRBs (Asai et al. 2000), and so if several bright XRBs are the source of the continuum photons, they must be located behind a significant amount of absorbing material that suppresses the photoionizing continuum.

Assuming the necessary absorbing material is provided by the collimating torus, we can estimate the continuum luminosity required to produce the observed line strengths. For an ionization parameter of ~ 700 and a column density of 10^{23} cm^{-2}, line luminosities of $\sim 10^{37}$ erg s^{-1} require a a continuum luminosity of at least $\sim 10^{40}$ erg s^{-1} (Kallman 1991). This would make the continuum source a member of the recently-discovered class of ultraluminous compact X-ray sources[4] and similar to the luminous X-ray point source seen near the center of M 82 (Matsumoto et al. 2001). Given the location of the ultraluminous source at the core of NGC 253, chances are high in this case that it is an intermediate mass, accreting black hole (IMBH).

5.3. A Buried AGN

If an IMBH could be lurking at the core of NGC 253, then might a low-luminosity AGN be lurking there as well? Interestingly, Mohan et al. (2002) find that, if they assume an AGN is responsible for producing the radio recombination line emission, the observed X-ray luminosity is 1,000 times less than that required to produce the ionizing photon flux. This deficiency in X-ray flux is easily explained if, in addition to intersecting the collimating torus, our line of sight to the central source is blocked by gas that is Compton thick, with column density of $\geq 10^{24}$ cm^{-2}. In this case, the hard X-ray power-law continuum could be explained as scattered continuum X-rays from the AGN. Comparisons to observations of Seyfert 2 galaxies with buried X-ray nuclei (Awaki et al. 2000) would then suggest thst the intrinsic X-ray luminosity is at least $\sim 10^{41}$ erg s^{-1}, which would make NGC 253 a true LLAGN. The relatively low luminosity compared to other AGN might then result from advection dominated accretion or the lack of sufficient fuel, which is possible if the AGN is turning on or off.

Our proposed geometry for the core of NGC 253 is shown in Figure 4. The central source, possibly an IMBH or LLAGN, sits at the kinematic center of the ~ 300 pc diameter collimating torus. The energy of the starburst has forced much of the gas that used to occupy this cavity into the base of the starburst-driven wind, clearing a path for X-rays to escape along the axis of the torus. These X-rays are scattered from and also photoionize the surrounding material. Additional obscuration is provided by a ring of starburst material that provides the radiation force to support the torus (Ohsuga & Umemura 1999). This material may be Compton thick. The high ionization parameter of the surrounding gas

[4]Sources with X-ray luminosities higher than 10^{38} erg s^{-1}, the Eddington luminosity of a 1.4 solar mass accreting neutron star.

suggests physical conditions that are similar to warm absorbers in Seyfert 1 galaxies, but in this case we would be seeing the region from the side, in emission, rather than face on, in absorption.

We have shown that the conditions at the center of NGC 253 provide fertile ground for studying the connection between starburst and AGN activity. The most definitive result is that the gas associated with the circumnuclear starburst is responsible for obscuring the central continuum source. This scenario has been predicted for the early stages of AGN formation (e.g., Sanders et al. 1988), but more importantly, it shows that the putative ~pc-scale molecular torus in Seyfert 2 galaxies is not the only mechanism by which an AGN-like continuum source can be hidden from our view. We speculate that NGC 253 is in an evolutionary state where it is transitioning between a starburst and AGN phase.

6. Conclusions

Chandra X-ray observations of the nearby starburst galaxy NGC 253 reveal what may be the beginnings or endings of AGN activity. The excellent spatial resolution allows us to isolate the torus that collimates the starburst-driven nuclear outflow, with an X-ray column density of $\sim 2 \times 10^{23}$ cm^{-2}. At the center of the torus, along with the evolved, circumnuclear starburst, is a source of hard X-rays with an unabsorbed, 2 to 10 keV luminosity of $\geq 10^{39}$ erg s^{-1}. We suggest that this ionizing source is an intermediate-mass black hole or a weakly accreting supermassive black hole. These data provide a unique snapshot of the complex interplay between starburst and AGN activity.

Future tests of the starburst-AGN scenario will require studying older starburst populations in nearby galaxies. In particular, it is important to look at normal stars in the optical or at X-ray binaries with *Chandra* in the more evolved, more AGN-like composite (Seyfert/starburst) galaxies.

These observations were made using the Chandra X-ray Observatory, operated by NASA and the Harvard-Smithsonian Astrophysical Observatory. The authors thank Tahir Yaqoob for supplying the photoionization model.

REFERENCES

Asai, K., Dotani, T., Nagase, F. and Mitsuda, K. 2000, ApJS, 131, 571

Awaki, H., Ueno, S., Taniguchi, Y. and Weaver, K. A. 2000, ApJ, 542, 175

Bautista, M. A. and Kallman, T. R. 2000, ApJ, 544, 581

Calzetti, D., Armus, L., Bohlin, R., Kinney, A., Koorneef, J., & Storchi-Bergmann, T. 2000, ApJ, 533, 682

Condon, J. 1992, ARA&A, 30, 575

Condon, J. J., Huang, Z.-P., Yin, Q. F. and Thuan, T. X. 1991, ApJ, 378, 65

Engelbracht, C. W., Rieke, M. J., Rieke, G. H., Kelly, D. M. and Achtermann, J. M. 1998, ApJ, 505, 639

Forbes, D. A., Polehampton, E., Stevens, I. R., Brodie, J. P. and Ward, M. J. 2000, MNRAS, 312, 689

Frayer, D. T., Seaquist, E. R. and Frail, D. A. 1998, AJ, 115, 559

Grimm, H.-J., Gilfanov, M. and Sunyaev, R. (2001astro.ph..9239)

Israel, F. P., White, G. J. and Baas, F. 1995, AA, 302, 343

Kaastra, J.S. 1992, An X-Ray Spectral Code for Optically Thin Plasmas (Internal SRON-Leiden Report, updated version 2.0)

Kallman, T. R. and McCray, R. 1982, ApJS, 50, 263.

Kallman, T. R. 1991, "Iron Line Diagnostics in X-ray Sources," eds. A. Treves, G. C. Perola, and L. Stella (Berlin:Springer-Verlag), 87

Levenson, N. A., Weaver, K. A. and Heckman, T. M. 2001, ApJ, 550, 230

Liedahl, D.A., Osterheld, A.L., and Goldstein, W.H. 1995, ApJL, 438, 115

Matsumoto, H. et al. 2001, ApJ, 547, L25

Mewe, R., Gronenschild, E.H.B.M., and van den Oord, G.H.J. 1985, A&AS, 62, 197

Mohan, N. R., Anantharamaiah, K. R. and Goss, W. M. 2002, ApJ, in press

Moran, E. C., Lehnert, M. D. and Helfand, D. J. 1999, ApJ, 526, 649

Mouri, H. and Taniguchi, Y. 2002, astro-ph/0201102

Norman, C. and Scoville, N. 1988, ApJ, 332, 124

Ohsuga, K. and Umemura, M. 1999, ApJ, 521, L13

Oliva, E., Origlia, L., Maiolino, R. and Moorwood, A. F. M. 1999, AA, 350, 9

Peng, R., Zhou, S., Whiteoak, J. B., Lo, K. Y. and Sutton, E. C. 1996, ApJ, 470, 821

Pietsch, W. et al., astro-ph/0010608

Quinlan, G. D. and Shapiro, S. L. 1990, ApJ, 356, 483

Sanders, D. B., Soifer, B. T., Elias, J. H., Neugebauer, G. and Matthews, K. 1988, ApJ, 328, L35

Strickland, D. K., Heckman, T. M., Weaver, K. A. & Dahlem, M. 2000, AJ, 120, 2965

Tremaine, S. D., Ostriker, J. P. and Spitzer Jr., L. 1975, ApJ, 196, 407

Turner, J. L. and Ho, P. T. P. 1985, ApJ, 299, L77

Ulvestad, J. S. and Antonucci, R. R. J. 1997, ApJ, 488, 621

Van Bever, J. and Vanbeveren., D. 2000, AA, 358, 462

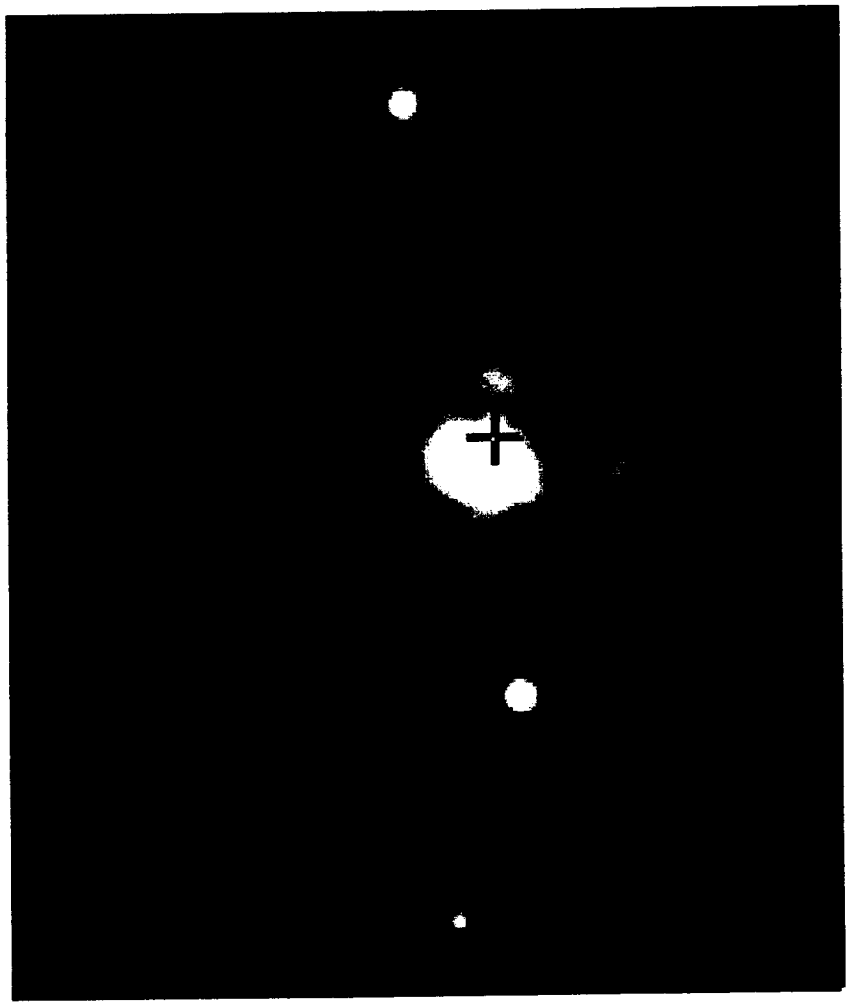

Fig. 1.— Three color composite Chandra X-ray image of the central 1.75′ by 2′ (1.4 kpc x 1.6 kpc) region of NGC 253, smoothed to achieve a local S/N of 3. Red, yellow and blue indicate the X-ray "colors" of 0.2–1.5 keV (soft), 1.5–4.5 keV (medium) and 4.5–8 keV (hard), respectively. The cross marks the position of the radio core (Turner and Ho 1985).

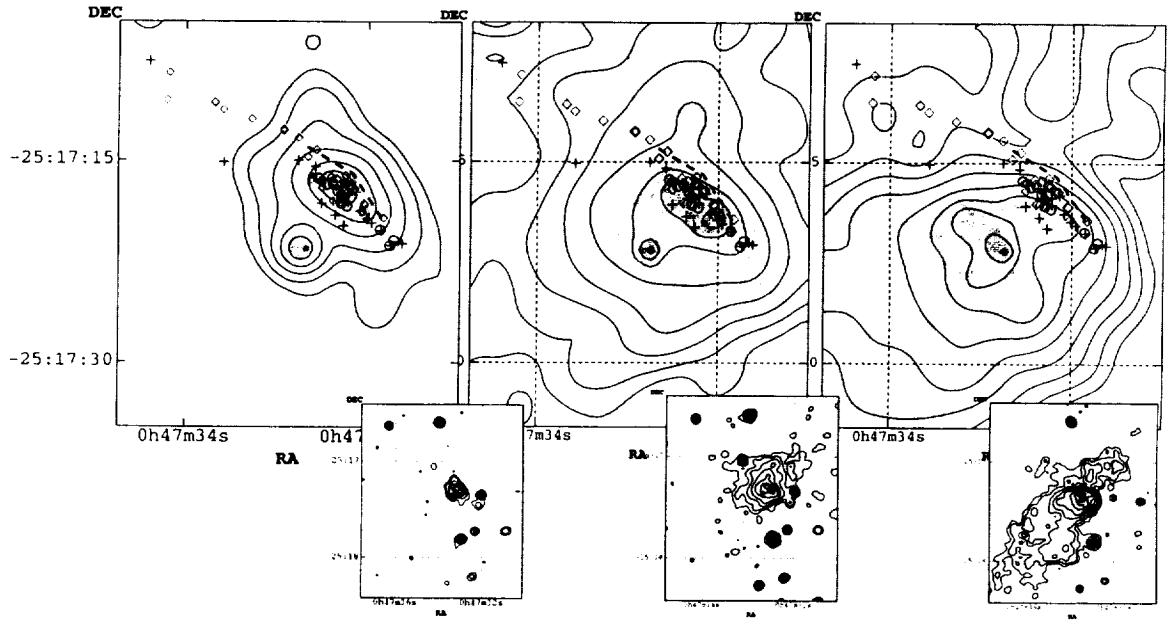

Fig. 2.— Hard, medium and soft X-ray images (the three energy bands that are combined to produce Figure 1) with data from other wavebands. Grey-scale represents the unbinned (0.5″ x 0.5″) and unsmoothed *Chandra* image. The thin black lines represent the brightness contours of the adaptively smoothed images. Contours are logarithmic and start at 2σ above the *local* background; the soft contours range from 0.1 to 14.0 counts/pixel; medium contours range from 0.04 to 21.0 counts/pixel; hard contours range from 0.03 to 11.0 counts/pixel. Crosses mark the compact radio sources (Ulvestad and Antonucci 1997). Circles represent compact OH maser features (Frayer, Seaquist and Frail 1998). Diamonds mark discrete optical and IR sources (Forbes et al. 2000). The inverted triangle marks the position of the radio nucleus (Turner and Ho 1985). The thick dashed line shows the approximate location of the dusty torus (Israel, White and Baas 1995; Dahlem et al. in prep.). Insets show the full smoothed images and contours overlaid, on a larger scale.

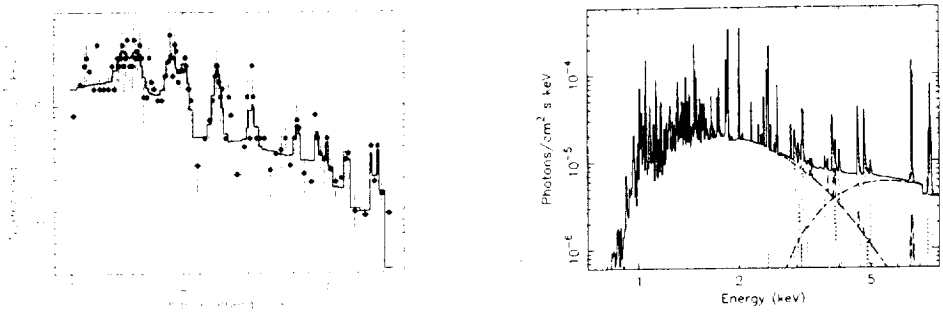

Fig. 3.— a) The *Chandra* spectrum of the galaxy core and best-fitting empirical model (solid line) that consists of a power law plus 12 Gaussian emission lines (Table 1). Data are grouped for illustration purposes such that each energy bin contains a minimum of 5 counts. b) Best-fitting model for the X-ray emission at the core of NGC 253 that consists of a low temperature thermal plasma and a heavily absorbed hard component ($N_{\rm H} = 2 \times 10^{23}$) that is a combination of a power law ($\Gamma = 1.9$) plus emission from a photoionized plasma with $\xi \sim 700$ (dotted lines).

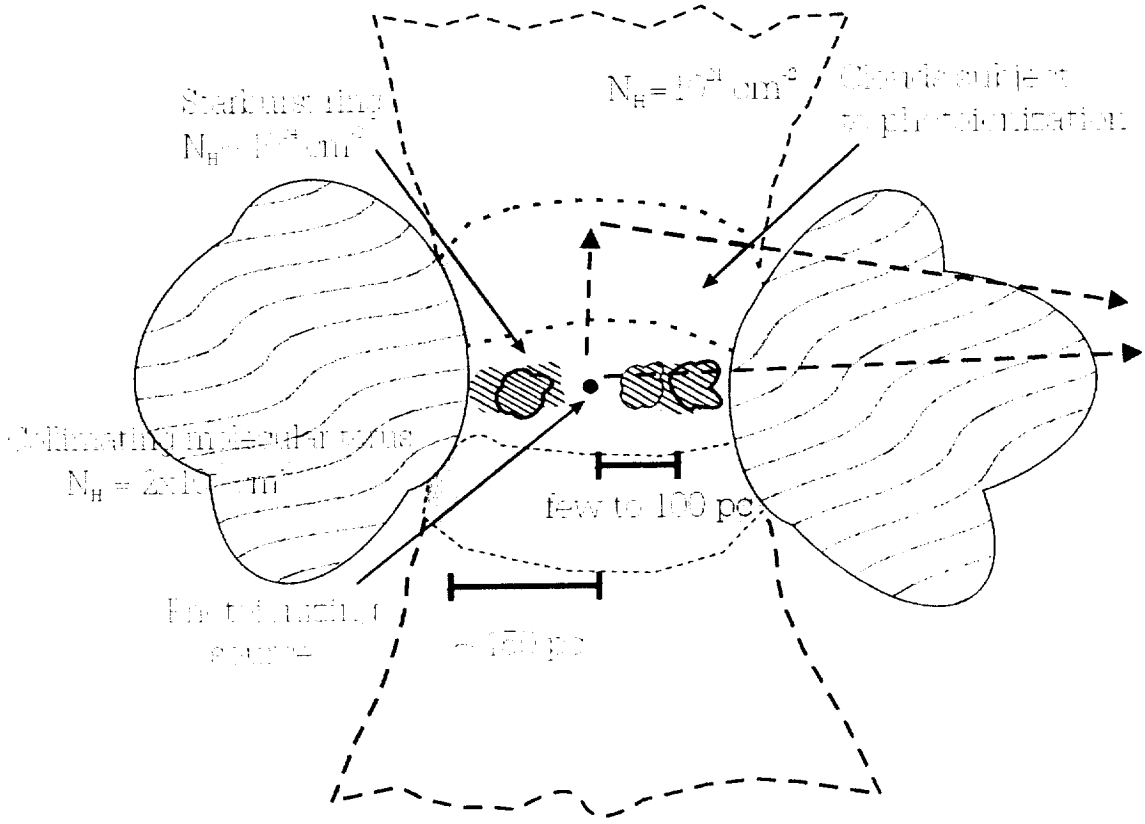

Fig. 4.— A cartoon of the central region of NGC 253.

Table 1. X-ray Emission Features as Individual Gaussians

Energy (keV)	norm[a] (10^{-6})	EW (eV)	Luminosity (10^{37} erg s^{-1})	ID
1.40±0.04	3.3(1.5-5.5)	106(50-175)	2.0	Mg XI
1.52±0.03	3.9(2.2-5.8)	136(76-203)	2.6	Fe XXII
1.86±0.02	5.1(3.5-7.5)	232(161-342)	4.2	Si XIII
2.02±0.03	4.3(2.7-6.3)	218(136-323)	3.7	Si XIV
2.46±0.02	7.2(4.8-9.8)	464(313-643)	7.7	S XV
3.05±0.05	2.5(1.0-4.6)	222(90-401)	3.9	S XVI - Ar XVII
4.08±0.08	1.5(0.4-3.2)	190(56-403)	3.2	Ca XIX-XX
4.61±0.08	1.5(0.4-3.3)	222(63-479)	3.5	Ar Rad Rec Cont ?
4.91±0.13	1.3(0.2-3.0)	215(25-478)	3.3	?
5.58±0.10	2.2(0.6-4.2)	410(120-800)	5.1	Ca Rad Rec Cont ?
6.50±0.07	3.9(1.6-7.6)	302(122-589)	1.1	Fe IV-XV
6.79(6.75-6.86)	5.9(2.8-10.2)	618(290-1,060)	1.8	Fe XXV

Note. — Data are unbinned and analyzed with the c-statistic. The continuum model is an absorbed power law with $\Gamma = 1.3$, $N_H = 0.32 \times 10^{22}$ cm^{-2} and a normalization of 4.9×10^{-5} photons keV^{-1} cm^{-2} s^{-1} at 1 keV.

[a]10^{-6} photons cm^{-2} s^{-1}.

Table 2. Fits to Chandra Spectrum of the Nucleus of NGC 253

#	Model	$N_{\rm H}1^a$	kT1^b	Z / logξ	$N_{\rm H}2^a$	Γ or kT2^b	χ^2	$F^c_{\rm obs}$	$F^c_{\rm unabs}$
1	M	0.9±0.3	$4.3^{+3.4}_{-2.0}$	1f/$\cdots$	$\cdots$	$\cdots$	72/32	3.8	4.2
2	M+M	1.8±0.2	1.1±0.2	1f /$\cdots$	$\cdots$	> 20.0	47/30	4.2	5.0
3	M+M	$2.0^{+0.2}_{-0.3}$	1.2±0.2	$7.5^{+12.0}_{-3.0}$ /$\cdots$	$\cdots$	$\cdots$/ 20.0f	40/29	4.5	5.5
4	M+P	$2.0^{+0.2}_{-0.3}$	1.2±0.2	1f /$\cdots$	$\cdots$	$-0.3^{+0.6}_{-1.5}$ /$\cdots$	34/35	6.8	7.9
5	M+M	$2.0^{+0.2}_{-0.3}$	1.2±0.2	1f /$\cdots$	45^{+16}_{-13}	$\cdots$/ 1.2f	31/30	4.3	69.4
6	M+P	$2.0^{+0.2}_{-0.3}$	1.2±0.2	1f /$\cdots$	18^{+10}_{-8}	1.9f /$\cdots$	31/30	5.1	11.4
7	M+P +Phot^d	$2.0^{+0.2}_{-0.3}$	$1.1^{+0.3}_{-0.1}$	1f / 2.6±0.5	20^{+13}_{-9}	1.7f /$\cdots$	26/27	12	23

Note. — Data are grouped to have at least 15 counts per bin. Models are M=Mekal plasma, P=Power law, Phot=Emission from cool, photoionized plasma. f=fixed parameter.

[a]Absorbing column density ($N_{\rm H}$) in units of 10^{22} cm^{-2}

[b]kT in units of keV.

[c]Flux is 2 – 10 keV in units of 10^{-13} ergs cm^{-2} s^{-1}.